UDC 539.3

Siberian Journal of Science and Technology. 2018, Vol. 19, No. 1, P. 27–36

MULTIGRID FINITE ELEMENTS IN THE CALCULATIONS OF MULTILAYER CYLINDRICAL SHELLS

A. D. Matveev[1*], A. N. Grishanov[2]

[1]Institute of Computational Modeling
50/44, Akademgorodok, Krasnoyarsk, 660036, Russian Federation
[2]Novosibirsk State Technical University
20, Karl Marx Av., Novosibirsk, 630073, Russian Federation
[*]E-mail: mtv241@mail.ru

An effective numerical method for calculating linearly elastic multilayer cylindrical shells under static loading implemented on the basis of Finite Element Method (FEM) procedures using the multilayer curved Lagrangian multigrid finite elements (MFE) of the shell type was proposed. Such shells are widely used in rocket-space and aircraft engineering. MFE are developed in local Cartesian coordinate systems based on small (basic) shell partitions that take into account their heterogeneous structure, irregular shape, combined loading and fixing. The stress strained state (SSS) in the MFE was described by the equations of the three-dimensional elasticity problem without using the additional kinematical and static hypotheses, which allow one to use MFE for the shells of various thicknesses to be calculated. The procedure of constructing the Langrage polynomials in local curvilinear coordinate systems used to develop the shell MFE is presented. The displacements in the MFE were approximated by the power and Lagrange polynomials of different orders. When constructing a n -grid finite element (FE), $n \geq 2$, n-nested grids were used. The fine grid was generated by the basic partition of the MFE; the other (coarse) grids were used to reduce its dimension. According to the method, the nodes of the coarse MFE grids are located on the common boundaries of the different modular layers of the shell. The proposed law of the expansion in the number of discrete models using MFE with a constant thickness, multiple of the shell thickness, provides a uniform and rapid convergence of approximate solutions, allowing one to frame solutions with a small error. Multigrid discrete models have $10^3 \ldots 10^6$ times less unknown MFE than the basic ones. The implementation of the MFE for multigrid models requires $10^4 \ldots 10^7$ times less computer storage space than for the reference models, which allows one using the proposed method to calculate some large shells. An example of calculating a multilayer cylindrical local loading shell of irregular shape was given. In the calculation, three-grid shell – type FE, developed on the basis of the reference models having from 2 million to 3.7 billion of the nodal MFE unknowns were used. To study the approximate solution convergence and error, a well-known numerical method was used.

Keywords: elasticity, cylindrical shells, composites, multigrid finite elements of shell type, Lagrange polynomials, small error.

Сибирский журнал науки и технологий. 2018. Т. 19, № 1. С. 27–36

МНОГОСЕТОЧНЫЕ КОНЕЧНЫЕ ЭЛЕМЕНТЫ В РАСЧЕТАХ МНОГОСЛОЙНЫХ ЦИЛИНДРИЧЕСКИХ ОБОЛОЧЕК

А. Д. Матвеев[1*], А. Н. Гришанов[2]

[1]Институт вычислительного моделирования СО РАН
Российская Федерация, 660036, г. Красноярск, Академгородок, 50/44
[2]Новосибирский государственный технический университет
Российская Федерация, 630073, г. Новосибирск, просп. К. Маркса, 20
[*]E-mail: mtv241@mail.ru

Предложен эффективный численный метод расчета линейно-упругих многослойных цилиндрических оболочек при статическом нагружении с применением многослойных криволинейных лагранжевых многосеточных конечных элементов (МнКЭ) оболочечного типа. Такие оболочки широко используются в ракетно-космической и авиационной технике. МнКЭ проектируются в локальных декартовых системах координат на основе мелких (базовых) разбиений оболочек, которые учитывают их неоднородную структуру, сложную форму, сложное нагружение и закрепление. Напряженное деформированное состояние в МнКЭ описывается уравнениями трехмерной задачи теории упругости без использования дополнительных кинематических и статических гипотез, что позволяет применять МнКЭ для расчета многослойных оболочек различной толщины. Показана процедура построения в локальных криволинейных системах координат полиномов Лагранжа, которые применяются при проектировании оболочечных МнКЭ. Перемещения в МнКЭ аппроксимируются степенными *и лагранжевыми полиномами различных порядков. При построении n -сеточного конечного элемента (КЭ), n ≥ 2, используют n вложенных сеток. Мелкая сетка порождена базовым разбиением МнКЭ, остальные n – 1 (крупные) сетки применяются для понижения его размерности. В предлагаемом методе узлы крупных сеток МнКЭ расположены на общих границах разномодульных слоев оболочки. Закон измельчения дискретных моделей, в которых используются МнКЭ с постоянной толщиной, кратной толщине оболочки, порождает равномерную и быструю сходимость приближенных решений, что дает возможность строить решения с малой погрешностью. Многосеточные дискретные модели имеют в 10^3–10^6 раз меньше узловых неизвестных, чем базовые. Реализация метода конечных элементов (МКЭ) для многосеточных моделей требует в 10^4–10^7 раз меньше объема памяти ЭВМ, чем для базовых, что позволяет использовать предложенный метод для расчета оболочек больших размеров. В приведенном расчете многослойной цилиндрической оболочки сложной формы, имеющей локальное нагружение, используются оболочечные трехсеточные КЭ, построенные на базовых моделях, которые имеют от 2 миллионов до 3,7 миллиарда неизвестных МКЭ. Для анализа сходимости приближенных решений используется известный численный метод.*

Ключевые слова: упругость, цилиндрические оболочки, композиты, многосеточные конечные элементы оболочечного типа, полиномы Лагранжа, малая погрешность.

Introduction. Finite Element Method (FEM) [1; 2] is widely used in the study of stress strained state (SSS) of elastic shells [3–6]. In the calculation of shells, constructing the curvilinear finite elements (FE) causes various difficulties [3], in particular, related to the fulfillment of conformality conditions, which is necessary for the convergence of finite element solutions [7]. These difficulties are largely due to the fact that to reduce the order of equations in the theory of shells, hypotheses are introduced, that impose certain restrictions on the fields of displacement, strain and stress [8–14], which generates irreducible errors in solutions and limits the applications of these theories. For example, in the work [15; 16] three-dimensional finite elements are considered with a given distribution of displacements through the thickness, given the compression of the shell. In the work [17] the review of the basic options of use of FEM for calculation of composite plates and covers in two-dimensional statement is presented. The attempts to calculate composite cylindrical shells with application of FE in the formulation of the three-dimensional problem of elasticity theory with account of their structure leads to systems of linear algebraic equations (SLAE) of the finite element method of high order (more 10^6). Application for such discrete shell models of calculation of ANSYS, NASTRAN etc. [3] is difficult. In addition, the solution obtained for the systems of high-order FEM equations contains a computational error, which is difficult to determine the exact value.

In this regard, there is a need to develop such variants of FEM, in which the composite cylindrical shell is considered in a three-dimensional formulation, but which lead to SLAE of a low order in compliance with the permissible level of SSS error values. In the works [18–20] calculations of composite cylindrical panels and shells with the help of multigrid finite element (MFE) are carried out, that was constructed using power polynomials.

In this paper, we propose an efficient numerical method of calculating linearly elastic multilayer cylindrical shells using a multilayer curvilinear Lagrangian MFE. Constructing n net finite element (FE), $n \geq 2$, n of enclosed grid is used. Small grids are made by basic splitting of MFE, the other $n-1$ (larger) grids are used to reduce its dimension. The aim of this work is to develop Lagrangian curved multilayer shell-type MFE. A procedure for constructing Lagrange polynomials of different orders in local curvilinear coordinates is proposed. In constructing approximate solutions a multi-layer Lagrangian, MFE shell with a constant thickness, a multiple of the thickness of the shell is used. The order of the Lagrange polynomial in thickness is taken by a multiple to the number of shell layers. Calculations show that the arrangement of nodes of large MFE grids on the common boundaries of different-modular shell layers provides homogenous and fast convergence of sequences of finite-element solutions, which allows to construct approximate solutions with low error. The proposed MFE are effective in calculating the SSS of multilayer cylindrical shells of different thicknesses, especially in the calculation of thin shells having a complex shape, the complex nature of the fixations and loads. Multilayer shells are widely used in rocket-space and aviation technology.

The advantages are as follows. Multilayer Lagrangian shell MFE:

– take into account the heterogeneous structure of the shells;

– describe the three-dimensional stress state in multi-layer shells;

– form multigrid discrete shell models, the dimension of which is much smaller than the dimensions of the base models;

– generate the numerical solution with fast convergence to accurate, which allows us to construct solutions with a small error.

Calculations show that application of the FEM for multigrid discrete models requires 10^3–10^7 time less computer memory than the base models need. The implementation of the proposed method on single-processor computers requires a small amount of time. To analyze the convergence of approximate solutions constructed for the initial problem, we use the well-known numerical method [2]. The implementation of this method is performed by constructing a sequence of approximate solutions for a similar test problem using MFE, which are used in solving the original problem. An example of calculating a 4-layer shell of complex shape using 4-layer Lagrangian shell three-grid FE is given. The results of the calculations show the high efficiency of the application of the proposed three-grid FE.

1. Homogeneous curvilinear single-grid FE. The procedure for constructing curvilinear homogeneous single-grid FE, which form a basic discrete model of the shell, is briefly considered as the example of FE V_e of the 1st order, located in the local Cartesian coordinate system $O_1x_1y_1z_1$ (fig. 1). For FE V_e designations are given: $h_x^e \times h_y^e \times h_z^e$ – characteristic sizes, $z_1O_1y_1$ – a symmetry plane, cd – an axis of a shell, R_1^e (R_2^e) – radius of curvature of the bottom (top) surface, h_z^e – thickness, h_y^e – length, $h_x^e = \alpha_e R_1^e$, α_e – an opening angle. The shape of the FE V_e is a straight prism with height h_y^e. Deformation of FE V_e is described by the equations of the three-dimensional problem of the theory of elasticity [1], shown in coordinate system $O_1x_1y_1z_1$. Using a first order polynomial (in the coordinate system $O_1x_1y_1z_1$), for FE V_e we define the stiffness matrix $\left[K_e^1\right]$ and the nodal force vector $\mathbf{P}_e^1$ with formulas [1; 2]

$$[K_e^1] = \int_{V_e} [B_e]^T [D_e][B_e] dV,$$
$$\mathbf{P}_e^1 = \int_{V_e} [N_e]^T \mathbf{F}_e dV + \int_{S_e} [N_e]^T \mathbf{q}_e dS, \quad (1)$$

where $[B_e]$, $[D_e]$ are the matrix of differentiation and modules of elasticity of the FE V_e; $\mathbf{F}_e$, $\mathbf{q}_e$ are the volume and surface forces vectors FE V_e; $[N_e]$ is the matrix of shape functions; V_e, S_e are the area and the surface of the FE V_e.

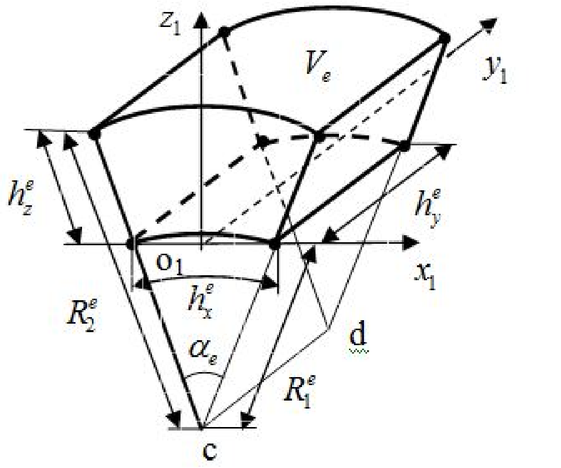

Fig. 1. Single-grid FE V_e

Рис. 1. Односеточный КЭ V_e

Note that the continuity of displacements is violated on the curvilinear boundaries of the FE V_e (fig. 1). However, as it's known [21], the implementation of continuous displacements at the boundaries of curvilinear FE is not a necessary condition for convergence of numerical solutions to the exact one. Calculations show that when the characteristic sizes of curved homogeneous FE V_e decrease, the numerical solutions converge to the exact ones. Procedures for the construction of homogeneous curvilinear single-grid FE of 2nd and 3rd order, which are geometrically similar to the form of FE V_e (fig. 1), are analogous to the procedure in § 1.

2. Multilayer curvilinear Lagrangian two-grid FE

The procedure of constructing multilayer curvilinear two-grid FE (TGFE) with the use of Lagrange polynomials is considered with the example of a three-layer TGFE V_a of the 3rd order with its thickness equal to h that is used in the calculation of 3-layer shells with the thickness h. In the calculation of m-layer shell m-layer Lagrangian TGFE of m-order in thickness are used. TGFE is located in a local Cartesian coordinate system $O_2x_2y_2z_2$ (fig. 2), its dimensions are $h_x^a \times h_y^a \times h$, h – thickness, h_y^a – length. Suppose that the bonds between the components of the inhomogeneous structure of TGFE are ideal. Basic partitioning of R_a TGFE, which consists of a homogeneous curvilinear FE V_e of the 1st order (fig. 1), takes into account in TGFE inhomogeneous structure, a complex type of loading and fastening, and generates a small curvilinear grid h_a, $e = 1, ..., M$, M is the total number of FE V_e. On the grid h_a we define the large curvilinear grid $H_a \subset h_a$, TGFE, the nodes of this grid are marked with dots, 64 nodes in fig. 2. Note that the nodes of the large grid H_a lie on the common boundaries of different-modular layers TGFE (fig. 2), in general they have different thickness. Suppose the axis O_1y_1 (fig. 1) is parallel to the axis O_2y_2 (fig. 2). Thus we can use a formula of relation between the nodal displacement vectors $\boldsymbol{\delta}_e^1$ $\boldsymbol{\delta}_e$, FE V_e, which correspond to the local Cartesian coordinate systems $O_1x_1y_1z_1$ and $O_2x_2y_2z_2$

$$\boldsymbol{\delta}_e^1 = [T_e]\boldsymbol{\delta}_e, \quad (2)$$

where $[T_e]$ is a square matrix of rotations [2], $e = 1, ..., M$.

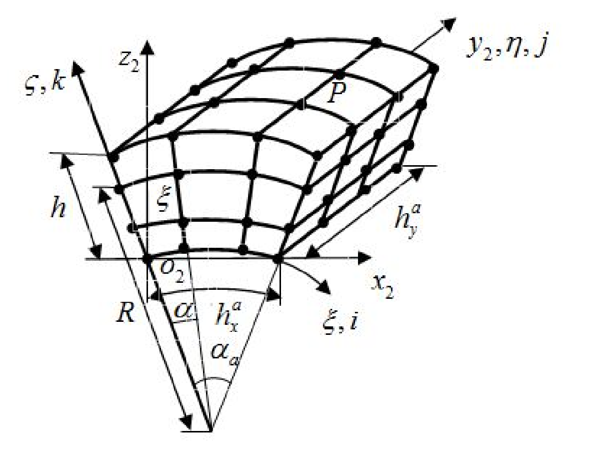

Fig. 2. Three-Layer TGFE V_a

Рис. 2. Трехслойный ДвКЭ V_a

We consider the construction of Lagrange polynomials in the local curvilinear coordinate system $O_2\xi\eta\varsigma$ on a large grid H_a (fig. 2). Suppose that the node $P(i,j,k)$ of grid H_a (dimensions $n_1 \times n_2 \times n_3$) has coordinates ξ_i, η_j, ζ_k, in fig. 2 $i = j = 3$, $k = 4$. Note that $y_2 = \eta$ for small opening angles α_a, TGFE we can see that $x_2 \approx \xi$, $z_2 \approx \zeta$. We have

$$x_2 = \xi, \quad y_2 = \eta, \quad z_2 = \zeta. \tag{3}$$

The base function N_{ijk} for a node $P(i,j,k)$ in the Cartesian coordinate system $O_2x_2y_2z_2$ using Lagrange polynomials $L_i(x_2),\ L_j(y_2),\ L_k(z_2)$ [2] is written in the form of

$$N_{ijk}(x_2,y_2,z_2) = L_i(x_2)L_j(y_2)L_k(z_2),$$

$$L_i(x_2) = \prod_{n=1,n\neq i}^{n_1} \frac{x_2 - x_{2,n}}{x_{2,i} - x_{2,n}},\ L_j(y_2) = \prod_{n=1,n\neq j}^{n_2} \frac{y_2 - y_{2,n}}{y_{2,j} - y_{2,n}}, \tag{4}$$

$$L_k(z_2) = \prod_{n=1,n\neq k}^{n_3} \frac{z_2 - z_{2,n}}{z_{2,k} - z_{2,n}},$$

where $x_{2,i}$, $y_{2,j}$, $z_{2,k}$ are the coordinates of the node $P(i,j,k)$ in the coordinate system $O_2x_2y_2z_2$.

For a point with a coordinate ξ lying on the cylindrical surface of the radius R, we have $\xi = \alpha R$, α is the angle for the coordinate ξ, fig. 3. Considering (3) the ratio of the form $\xi = \alpha R$, $\xi_i = \alpha_i R$ in (4), we obtain $N_{ijk}(\alpha,\eta,\zeta) = L_i(\alpha)L_j(\eta)L_k(\zeta)$, where $L_i(\alpha)$, $L_j(\eta)$, $L_k(\zeta)$ are the Lagrange polynomials, having the form

$$L_i(\alpha) = \prod_{n=1,n\neq i}^{n_1} \frac{\alpha - \alpha_n}{\alpha_i - \alpha_n},\quad L_j(\eta) = \prod_{n=1,n\neq j}^{n_2} \frac{\eta - \eta_n}{\eta_j - \eta_n},$$
$$L_k(\zeta) = \prod_{n=1,n\neq k}^{n_3} \frac{\zeta - \zeta_n}{\zeta_k - \zeta_n}. \tag{5}$$

It is convenient to use Lagrange polynomials (5) in calculations. Displacement functions u_a, v_a, w_a TGFE, constructed on the grid H_a using Lagrange polynomials (5), are presented in the form of

$$u_a = \sum_{\beta=1}^{n_0} N_\beta q_\beta^u, \quad v_a = \sum_{\beta=1}^{n_0} N_\beta q_\beta^v, \quad w_a = \sum_{\beta=1}^{n_0} N_\beta q_\beta^w, \tag{6}$$

where q_β^u, q_β^v, q_β^w, N_β are displacements and shape function of the β node of grid H_a, $n_0 = n_1n_2n_3$, in the present case $n_0 = 64$ (fig. 2).

Using (1), (2), the stiffness matrix $[K_e]$ and the nodal forces vector P_e of FE V_e in the coordinate system $O_2x_2y_2z_2$, we present $[K_e] = [T_e]^T[K_e^1][T_e]$, $\mathbf{P}_e = [T_e]^T\mathbf{P}_e^1$ [1]. The functional of the full potential energy Π_a of the basic partition of the R_a TGFE V_a can be written in the form of

$$\Pi_a = \sum_{e=1}^{M}\left(\frac{1}{2}\boldsymbol{\delta}_e^T[K_e]\,\boldsymbol{\delta}_e - \boldsymbol{\delta}_e^T\mathbf{P}_e\right). \tag{7}$$

Using small partitions R_a, the functional (7) has a high dimension and generates a multinodal FE with a large number of nodal unknowns, which is not effective for practice. To reduce the dimension of the functional (7), we use the following procedure. Using (6), the vector of nodal displacements $\boldsymbol{\delta}_e$ FE V_e is shown through the vector of nodal displacements $\boldsymbol{\delta}_a$ of large grid H_a TGFE V_a

$$\boldsymbol{\delta}_e = [A_e^a]\boldsymbol{\delta}_a, \tag{8}$$

where $[A_e^a]$ is a rectangular matrix $e = 1,...,M$.

Substituting (8) in (7) and following the principle of the minimum of total potential energy for TGFE V_a, $\partial\Pi_a(\boldsymbol{\delta}_a)/\partial\boldsymbol{\delta}_a = 0$ we obtain a ratio $[K_a]\boldsymbol{\delta}_a = \mathbf{F}_a$ corresponding to the equilibrium state of TGFE V_a, where

$$[K_a] = \sum_{e=1}^{M}[A_e^a]^T[K_e][A_e^a],\ \ \mathbf{F}_a = \sum_{e=1}^{M}[A_e^a]^T\mathbf{P}_e. \tag{9}$$

The matrix $[K_a]$ is called the stiffness matrix, $\mathbf{F}_a$ is nodal forces vector of TGFE V_a. Note that the functions u_a, v_a, w_a are used only to reduce the dimension of the functional (7), the large grid H_a determines the dimension of the TGFE V_a, which is less than the dimension of the base partition R_a.

Note 1. By virtue of (8) the dimension of the vector $\boldsymbol{\delta}_a$ (i. e. the dimension of the TGFE V_a) does not depend on the M which is the total number of FE V_e constituting the TGFE V_a. Consequently, it is possible to use arbitrarily small base partitions R_a, which allows to take into account the heterogeneous and micro-homogeneous structure of the TGFE V_a.

Note 2. In formula (9), matrices $[K_e]$, $\mathbf{P}_e$, $[A_e^a]$ are constructed taking into account the curvilinear form of the base FE V_e (see formula (1)), which represent the region TGFE V_a geometrically accurately. Consequently, the matrices $[K_a]$, $\mathbf{F}_a$ are also determined taking into account the curvilinear form of the TGFE V_a.

Note 3. The determination of the stresses in TGFE V_a can be shown as follows. Let the vector $\boldsymbol{\delta}_a$ be found. With the help of the formulas (8), (2) we find vectors $\boldsymbol{\delta}_e$, $\boldsymbol{\delta}_e^1$ nodal displacements of FE V_e ($e = 1, ..., M$) respectively, in coordinate systems $O_2x_2y_2z_2$ and $O_1x_1y_1z_1$. Using vector $\boldsymbol{\delta}_e^1$ we count the tension in the FE V_e with algorithms of the finite element method [1; 2].

Note 4. Lagrange polynomials are used in Lagrangian TGFE polynomials, determined by formulas (5), which have the order of the polynomial multiple of the number of layers in the thickness of the shell on the coordinate z (i. e. ζ). The calculations show that the location of the nodes of the large grid H_a TGFE at the boundaries of heterogeneous layers provides a homogenous and rapid convergence of sequences of approximate solutions.

The procedures of constructing composite Lagrangian TGFE of *n*-order, geometrically similar to TGFE V_a (fig. 2), with the application of Lagrange polynomials of n-order, are similar to the procedure of § 2.

Calculations show that by increasing the dimensions of the basic partitions of TGFE (i. e., by increasing the number *M*), the time spent on the construction of matrices $[K_a]$ и $\mathbf{F}_a$ and formulas (9) significantly increase. In this case, it is advisable to apply 3-grid finite elements, for the construction of which less time is required and which generate the discrete shell model of lower dimension than TGFE.

3. Multilayer curvilinear Lagrangian three-grid FE.

The procedure of constructing curvilinear three-grid FE (ThGFE) with the use of Lagrange polynomials is considered by the example of a six-layer ThGFE V_b of the 6-th order with its thickness h_z^b, that is used in the calculation of 6-layer shells with thickness h, where $h = h_z^b$. In the calculation of *m*-layer shell *m*-layer Lagrangian ThGFE of *m*-order thickness are used. ThGFE V_b with the size $h_x^b \times h_y^b \times h_z^b$ is located in the local Cartesian coordinate system $O_3x_3y_3z_3$ (fig. 3).

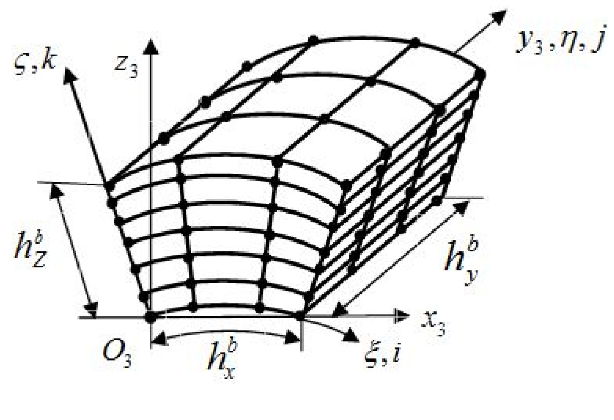

Fig. 3. Six-Layer, ThGFE V_b

Рис. 3. Шестислойный ТрКЭ V_b

The area of ThGFE consists of N curved 6-ply TGFE V_a^n with thickness *h*, $n = 1, ..., N$ that geometrically accurately represent the area of ThGFE. TGFE V_a^n make the partition R_b. The large grids H_a TGFE form a small grid h_b ThGFE. On the grid h_b we define large grid of $H_b \subset h_b$ ThGFE. The nodes of the large grid H_b marked with points (112 nodes) lie on the common boundaries of different-modular layers of ThGFE (fig. 3).

Suppose that the axis O_2y_2 of ThGFE (fig. 2) is parallel to the axis O_3y_3 (fig. 3). Suppose that $\boldsymbol{\delta}_n^a$, $\mathbf{q}_n^a$ are the vectors of nodal displacements, $[K_a^n]$, $[M_n^a]$ are the stiffness matrices and $\mathbf{F}_n^a, \mathbf{P}_n^a$ are the vectors of nodal forces TGFE V_n^a responsible for the coordinate systems $O_2x_2y_2z_2$ and $O_3x_3y_3z_3$, $n = 1, ..., N$ respectively. According to the FEM [1] we define the following formula: $\boldsymbol{\delta}_n^a = [T_n^a]\,\mathbf{q}_n^a$, where $[T_n^a]$ is the rotations matrix [2], $[M_n^a] = [T_n^a]^T[K_n^a][T_n^a]$, $\mathbf{P}_n^a = [T_n^a]^T\,\mathbf{F}_n^a$. Taking into account these relations, the total potential energy of the Π_b ThGFE V_b, i. e. the partition of R_b, is presented in the form of

$$\Pi_b = \sum_{n=1}^{N}\left(\frac{1}{2}\left(\mathbf{q}_n^a\right)^T\left[M_n^a\right]\mathbf{q}_n^a - \left(\mathbf{q}_n^a\right)^T\mathbf{P}_n^a\right). \qquad (10)$$

Functions of the displacements u_p, v_p, w_p ThGFE V_b on the large grid H_b, using Lagrange polynomials are presented in the form of

$$u_p = \sum_{\beta=1}^{n_0} N_\beta q_\beta^u,\quad v_p = \sum_{\beta=1}^{n_0} N_\beta q_\beta^v,\quad w_p = \sum_{\beta=1}^{n_0} N_\beta q_\beta^w, \qquad (11)$$

where q_β^u, q_β^v, q_β^w, N_β are displacements and shape function of the β node of grid H_b, $n_0 = n_1n_2n_3$, in this case $n_0 = 112$ (fig. 3).

To reduce the dimension of the functional (10) we use functions (11). Let's denote: $\boldsymbol{\delta}_b$ is the vector of nodal displacements of a large grid H_b. Expressing the nodal displacements of vector $\mathbf{q}_n^a$ TGFE V_n^a through the nodal displacement of vector $\boldsymbol{\delta}_b$ of the grid H_b ThGFE V_b, we can see the equality

$$\mathbf{q}_n^a = \left[A_n^b\right]\boldsymbol{\delta}_b, \qquad (12)$$

where $[A_n^b]$ is a rectangular matrix, $n = 1, ..., N$.

Using (12) in (10) and minimizing functional Π_b in displacement of $\boldsymbol{\delta}_b$, we obtain the ratio for the ThGFE V_b $[K_b]\boldsymbol{\delta}_b = \mathbf{F}_b$ that corresponds to its equilibrium state, where

$$[K_b] = \sum_{n=1}^{N}[A_n^b]^T[M_n^a][A_n^b],\ \mathbf{F}_b = \sum_{n=1}^{N}[A_n^b]^T\,\mathbf{P}_n^a. \qquad (13)$$

The matrix $[K_b]$ will be called the stiffness matrix, $\mathbf{F}_b$ is the vector of nodal forces ThGFE V_b. Note that the large grid H_b determines the dimension of the ThGFE V_b, which is less than the partition dimension R_b consisting of the TGFE V_n^a.

Note 5. By virtue of (12) the dimension of the vector $\boldsymbol{\delta}_b$ (i. e. the dimension of the ThGFE V_b) does not depend on the total number of TGFE V_n^a components of ThGFE. This means that the splitting of a ThGFE V_b into a TGFE V_n^a and, consequently, into single-grid FE V_e (see § 2) can be arbitrarily small, which allows to describe with arbitrarily small error the three-dimensional stress state in the ThGFE taking into account its inhomogeneous structure.

Note 6. Note that the number of layers of TGFE may be less than the number of layers of the shell. For example, constructing six-layered ThGFE you can use a three-layered TGFE (fig. 2) or two-layered TGFE. As calculations show, this leads to a decrease in time costs with a minor change in the error of the solution.

In the formula (13), matrices $[M_n^a]$, $\mathbf{P}_n^a$, $[A_n^b]$ are constructed taking into account the curvilinear form of TGFE V_n^a (see § 2), which geometrically represent the area accurately, ThGFE V_b. Consequently, the matrices $[K_b]$, $\mathbf{F}_b$ are also determined taking into account the curvilinear form of the ThGFE V_b.

The procedure of determining stresses in the ThGFE V_b is similar to the procedure for determining stresses in the TGFE.

Using ThGFE, according to the procedure similar to § 3, we construct four-grid FE, and the k grid of FE, $k \geq 4$. Note that the k grid generate a discrete FE shell model of lower dimension than the $k-1$ FE grid. The described method can be used to calculate multilayer shells with layers of different thicknesses.

Small enough partitions of composite shells are presented as homogeneous MFE, which are designed according to the procedures similar to § 1–3.

4. The results of numerical experiments. Consider the problem of deformation of a four-layered elastic cylindrical shell V_0 of a complex shape with length $2L$. The shell, clamped from two ends, is located in the Cartesian coordinate system $Oxyz$. When $y = 0;\ 2L$, displacement $u = v = w = 0$. The radius of the shell on the median surface $R = 2.0$ m, the thickness of the shell $h = 0.03$ m, length $2L = 12.0$ m, i. e V_0 is a thin shell with large geometric dimensions. The left symmetrical part of the shell is shown in fig. 4. Point A lies at the intersection of the planes Oyz and $y = L$ on the top surface of the shell. Shell layers are isotropic homogeneous bodies. The upper and lower layers have $h/12$ thickness, the inner 2 layers have $5h/12$. The Young's modules of 4 layers (starting from the bottom) are equal to: 10, 3, 5, 20 GPA, respectively. Poisson's ratio is 0.3. There is a uniformly distributed tensile radial load $q = 0.05$ MPa (fig. 4) on the outer surface of the shell $3L/4 \leq y \leq L$ with the opening angle $\alpha = \pi/2$, which is symmetrical to the planes Oyz and $y = L$. In the area of the shell clamps there are cutouts symmetrical to the plane Oyz, the opening angle of each cut is equal to the $\pi/2$ length is $L/4$ (fig. 4). As the shape, loading and fastening of the shell are symmetrical to the planes Oyz and $y = L$, we use 1/4 of the shell in the calculations.

The basic discrete model R_n^0 of the shell consists of a curved homogeneous single grid FE of the 1st order V_e^n, geometrically similar to FE V_e (fig. 1). The model grid R_n^0 has a dimension of $m_n^1 \times m_n^2 \times m_n^3$, where

$$m_n^1 = 324n + 1,\ \ m_n^2 = 324n + 1,$$
$$m_n^3 = 12n + 1,\ \ n = 1,\ ...,10, \tag{14}$$

m_n^1 is the dimension of the circular coordinate; m_n^2 – the axis Oy, m_n^3 – axis Oz. Characteristic sizes h_{xn}^e, h_{yn}^e, h_{zn}^e FE V_e^n are defined by the following formulas

$$h_{xn}^e = h_{x1}^e / n,\ \ h_{yn}^e = h_{y1}^e / n,$$
$$h_{zn}^e = h_{z1}^e / n,\ \ n = 1,\ ...,10, \tag{15}$$

where h_{x1}^e, h_{y1}^e, h_{z1}^e are characteristic dimensions of FE V_e^1 of the 1st order corresponding to the discrete model R_1^0, where $h_{x1}^e = \alpha_1 R_e$, $h_{y1}^e = L/324$, $h_{z1}^e = h/12$, $\alpha_1 = \pi/324$, R_e is the radius of the lower cylindrical surface FE V_e^1.

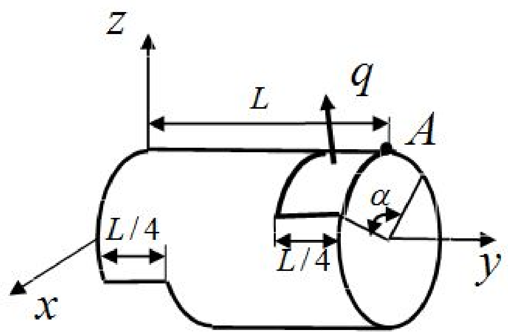

Fig. 4. Left symmetric part of the shell V_0

Рис. 4. Левая симметричная часть оболочки V_0

On base models R_n^0, $n = 1,\ ...,10$ we construct multigrid discrete models R_n of shell V_0 consisting of Lagrangian shell ThGFE with sizes $81h_{xn}^e \times 81h_{yn}^e \times h$ where $h = 12nh_{zn}^e$. For all basic discrete models, ThGFE have a fixed size coordinate z which is equal to the thickness of the shell h. ThGFE are constructed on the procedure shown in § 3 and consist of Lagrangian TGFE with dimensions $9h_{xn}^e \times 9h_{yn}^e \times h$, according to the procedure shown in § 2.

The ThGFE uses Lagrange polynomials defined by the formulas (5), which have the third order of the polynomial by coordinates *x*, *y*, and the forth order by coordinate z, which corresponds to the number of layers in the thickness of the shell. As shown by numerical calculations, if the nodes of large grids H_a and H_b of two-grid and three-grid FE lie on the common boundaries of multimodulus layers, discrete models R_n provide even and fast convergence of a sequence of finite element solutions.

The results of the calculations for discrete models R_n are given in tab. 1, where we see: w_n, σ_n are maximum radial displacement and equivalent stress for the model R_n, $n = 6, ..., 10$. We can find the stress σ_n with the 4th strength theory. As you know, using the maximum equivalent stress the factors of safety of structures are determined. We find the values $\delta_{\sigma,n}(\%)$, $\delta_{w,n}(\%)$ with the formulas

$$\delta_{\sigma,n}(\%) = 100\ \% \cdot |\sigma_n - \sigma_{n-1}| / \sigma_n ,$$

$$\delta_{w,n}(\%) = 100\ \% \cdot |w_n - w_{n-1}| / w_n , \quad n = 2, ..., 10 .$$

The nature of changes in values $\delta_{w,n}(\%)$, $\delta_{\sigma,n}(\%)$ (tab. 1) shows rapid convergence of the equivalent stresses σ_n and displacements w_n. Since the values for the model R_{10} are small, $\delta_{w,10} = 0.00116179$, $\delta_{\sigma,10} = 0.00719947$ it can be considered from the point of view of engineering practice that the displacement of $w_{10} = 30.289362$ mm and $\sigma_{10} = 31.371908$ MPa are made with low error, i. e., w_{10}, σ_{10} are little different from the exact (see § 5).

The dimension of the underlying discrete model R_{10}^0 is 3722110998 (more than 3.7 billion), the width of the tape of the system equations (SE) FEM is 1176610 (over 1.1 million). Multigrid model R_{10} has 203090 nodal unknowns, the width of the tape SE FEM is equal to 5445. Application of the FEM for the multigrid model R_{10} requires 3960366 (approximately 3.96 million) less times than the amount of computer memory of the base model R_{10}^0.

5. The study of the convergence of approximate solutions. To study the convergence of approximate solutions constructed using the new MFE, we use the following numerical method, the brief essence of which is shown below. With the kind of new MFE that are used in the solution of the original problem (see § 4), the similar (test) problem with known exact solution u_0 is solved. Suppose that $\| u_0 - u_h \| \to 0$ when $h \to 0$, where u_h is the solution of the test problem, constructed with the help of a family of new MFE, h is the characteristic size of MFE. Then we consider that the solutions constructed with the help of a family of new MFE and for the initial problem converge in the limit ($h \to 0$) to the exact one.

We consider the deformation of a 4-layer cylindrical shell V_1 as a test problem, which is located in the Cartesian coordinate system $Oxyz$, to have the same geometric dimensions, fastening conditions and elastic modules as the shell V_0 in § 4. However, the shell V_1 has no cutouts. When $3L/4 \le y \le 5L/4$ the radial tensile uniform load of $p = 0.1$ MPa acts on the outer surface of the shell V_1, i. e. axisymmetric three-dimensional stress state is realized in the shell V_1 [1].

As you know [1], the sequence of approximate solutions of the axisymmetric problem, constructed by MFE with the use of standard FE, which are homogeneous rings with a rectangular cross-section, in the limit (when $h_m \to 0$ h_m is the characteristic size of the standard FE) converge to the exact solution. Calculations are carried out for discrete models Q_n, $n = 1, ..., 14$, shell V_1. The results of calculations are given in tab. 2 for models Q_n where, $n = 7, ..., 14$, w_n^0, σ_n^0 are the deflection and equivalent voltage at the point A (fig. 4), dimensions of models Q_n are given in the plane Oyz. The parameters of $\delta_{w,n}^0(\%)$, $\delta_{\sigma,n}^0(\%)$ are determined by the formulas

$$\delta_{w,n}^0(\%) = 100\ \% \cdot |w_n^0 - w_{n-1}^0| / w_n^0 ,$$
$$\delta_{\sigma,n}^0(\%) = 100\ \% \cdot |\sigma_n^0 - \sigma_{n-1}^0| / \sigma_n^0 , \quad n = 2, ..., 14. \tag{16}$$

Table 1

Displacements w_n and equivalent stresses σ_n for models R_n

R_n	R_6	R_7	R_8	R_9	R_{10}
w_n	30.032632	30.136577	30.205840	30.254172	30.289362
$\delta_{w,n}(\%)$	0.550568	0.344913	0.229303	0.159753	**0.116179**
σ_n	30.074687	30.544130	30.881125	31.146047	31.371908
$\delta_{\sigma,n}(\%)$	2.374768	1.536934	1.091265	0.850580	**0.719947**

Table 2

Displacements w_n^0 and equivalent stresses σ_n^0 for models Q_n

N	Dimensions of models	$w_n^0 \cdot 10^3$, м	$\delta_{w,n}^0(\%)$	σ_n^0, MPa	$\delta_{\sigma,n}^0(\%)$
7	2269×43	2.24419205	0.0001359	21.9642981	0.0006719
8	2593×49	2.24419400	0.0000868	21.9641839	0.0005199
9	2917×55	2.24419529	0.0000574	21.9640928	0.0004147
10	3241×61	2.24419632	0.0000458	21.9640199	0.0003319
11	3565×67	2.24419706	0.0000329	21,.9639594	0.0002754
12	3889×73	2.24419754	0.0000213	21.9639074	0.0002367

End of table 2

N	Dimensions of models	$w_n^0 \cdot 10^3$, м	$\delta_{w,n}^0(\%)$	σ_n^0, MPa	$\delta_{\sigma,n}^0(\%)$
13	4213×79	2.24419797	0.0000147	21.9638637	0.0001989
14	4537×85	**2.24419832**	0.0000155	**21.9638261**	0.0001711

Table 3

Displacements w_n^p and stresses σ_n^p for models R_n

n	$w_n^p \cdot 10^3$, м	$\delta_{w,n}^p(\%)$	σ_n^p, MPa	$\delta_{\sigma,n}^p(\%)$
7	2.24416383	0.0001038	21.9641016	0.0060703
8	2.24416590	0.0000922	21.9649716	0.0039608
9	2.24416869	0.0001243	21.9655875	0.0028039
10	2.24417150	0.0002810	21.9660517	0.0021132
11	2.24417898	0.0003333	21.9664194	0.0016739
12	2.24418121	0.0000993	21.9667143	0.0013424
13	2.24418263	0.0000632	21.9669569	0.0011043
14	**2.24418427**	0.0000730	**21.9671598**	0.0009236

The nature of the values change of $\delta_{w,n}^0(\%)$, $\delta_{\sigma,n}^0(\%)$ shows the rapid convergence of stresses σ_n^0 and displacements w_n^0 to the exact solution w_0, σ_0 of the axisymmetric problem [1]. As the sizes, $\delta_{w,14}^0 = 0.000000155$ $\delta_{\sigma,14}^0 = 0.000001711$ are sufficiently small, the displacement of $w_{14}^0 = 2.24419832 \cdot 10^{-3}$ m and the equivalent stress $\sigma_{14}^0 = \ = 21.9638261$ MPa can be considered as the exact solution, i. e. we believe $w_0 = w_{14}^0$, $\sigma_0 = \sigma_{14}^0$.

We consider the solution of this axisymmetric MFE problem with the use of FE, which were used in solving the problem in § 4. We construct approximate solutions of the axisymmetric problem using the laws of grinding (14), (15) of basic partitions. The results of calculations are given in the tab. 3, where, w_n^p, σ_n^p is the deflection and equivalent stress at the point A for a multigrid discrete model R_n, $n = 7, ..., 14$. The parameters $\delta_{w,n}^p(\%)$, $\delta_{\sigma,n}^p(\%)$ are determined by formulas similar to formulas (16). The nature of the change in values $\delta_{w,n}^p(\%)$, $\delta_{\sigma,n}^p(\%)$ demonstrates the rapid convergence of stresses σ_n^p and displacements w_n^p to the limit values w_0^p, σ_0^p. The errors for displacement w_{14}^p and stress σ_{14}^p $\delta_w(\%) = 100\ \% \cdot | w_{14}^0 - w_{14}^p | / w_{14}^0$, $\delta_\sigma(\%) = 100\ \% \times \times | \sigma_{14}^0 - \sigma_{14}^p | / \sigma_{14}^0$, respectively, are equal to 0.00062828 % 0.0151749 %. In tab. 2, 3 values w_{14}^0, σ_{14}^0, w_{14}^p, σ_{14}^p, are marked in bold. From the point of view of engineering practice, because of the smallness of the values $\delta_w(\%)$, $\delta_\sigma(\%)$, we can assume that $w_0^p = w_0$, $\sigma_0^p = \sigma_0$. Then we can conclude that the proposed ThGFE generate solutions σ_n^p, w_n^p that in the limit (at $n \to \infty$) tend (from the point of view of engineering practice) to the exact solution of the axisymmetric problem.

The shell V_0 considered in § 4 differs from the shell V_1 considered in § 5 by the presence of cutouts and the method of applying the load, with full coincidence of the dimensions, boundary conditions and physical characteristics of the shells. In addition, when constructing sequences of approximate solutions for the initial and test problems, the same family of proposed ThGFE is used. Therefore, it can be assumed that the proposed shell ThGFE, which provide uniform convergence of approximate solutions for the test problem (for the shell V_1), generate solutions w_n, σ_n that in the limit (at $n \to \infty$) will converge (from the point of view of engineering practice) to the exact values of displacement and equivalent stress for the original problem (for the shell V_0), see § 4.

Conclusion. In this work we propose a numerical method of calculation of multilayered linear elastic cylindrical thin and medium-thickness shells with the use of curvilinear Lagrangian shell type MFE. Application of the MFE for multigrid discrete shell models requires much less computer memory than the base models, which allows to construct solutions with a small error and can explore SSS of shells of large geometric dimensions. The above calculations show the high efficiency of the proposed curvilinear Lagrangian shell MFE in the analysis of three-dimensional SSS multilayer shells.

References

1. Zenkevich O. *Metod konechnykh elementov v tekhnike* [The finite element method in engineering science]. Moscow, Mir Publ., 1975, 541 p.

2. Norri D., Zh. de Friz. *Vvedenie v metod konechnykh elementov* [An Introduction to Finite Element Analysis]. Moscow, Mir Publ., 1981, 304 p.

3. Golovanov A. I., Tyuleneva O. I., Shigabutdinov A. F. *Metod konechnykh elementov v statike i dinamike tonkostennykh konstruktsiy* [Finite Element Method in statics

and dynamics of thin-wall constructions]. Moscow, Fizmatlit Publ., 2006, 392 p.

4. Klochkov Yu. V., Nikolayev A. P., Shubovich A. A. *Analiz napryazhenno-deformirovan- nogo sostoyaniya obolochek vrashcheniya v geometricheski nelineynoy postanovke pri razlichnykh variantakh interpolyatsii peremeshcheniy* [Analysis of stress-strain state of rotation shells in geometrically non-linear setting with various variants of movement interpolation]. Volgograd, Volgogradsky GAU Publ., 2013, 152 p.

5. Kiselev A. P. [Calculation of thin shells for strength to resist three-dimensional setting, without simplifying hypotheses]. *Izv. vuzov, ser. Stroitel'stvo.* 2008, No. 1, P. 18–23 (In Russ.).

6. Kiselev A. P., Gureeva N. A., Kiseleva R. Z. [Calculating multilayer rotation shells and plates using volume finite elements]. *Izv. vuzov, ser. Stroitel'stvo.* 2010, No. 1, P. 106–112 (In Russ.).

7. Bate K., Wilson E. *Chislennye metody analiza i metod konechnykh elementov* [Numerical methods in finite element analysis]. Moscow, Stroyizdat Publ., 1982, 448 p.

8. Bolotin V. V., Novichkov Yu. N. *Mekhanika mnogosloynykh konstruktsiy* [Mechanics of multilayer structures]. Moscow, Mashinostroenie Publ., 1980, 375 p.

9. Golushko S. K., Nemirovskiy Yu. V. *Pryamye i obratnye zadachi mekhaniki uprugikh kompozitnykh plastin i obolochek vrashcheniya* [Direct and inverse problems of mechanics of elastic composite plates and shells of revolution]. Moscow, Fizmatlit Publ., 2008, 432 p.

10. Ahmed A., Kapuria S. A four-node facet shell element for laminated shells based on the third order zigzag theory. *Composite Structures.* 2016, Vol. 158, P. 112–127.

11. Carrera E., Pagani A. Valvano S. Shell elements with through-the-thickness variable kinematics for the analysis of laminated composite and sandwich structure. *Composites Part B: Engineering.* 2017, Vol. 111, P. 294–314.

12. Yasin M. Y., Kapuria S. An efficient layerwise finite element for shallow composite and sandwich shells. *Composite Structures.* 2013, Vol. 98, P. 202–214.

13. Cinefra M., Carrera E. Shell finite elements with different through-the-thickness kinematics for the linear analysis of cylindrical multilayered structures. *Int. J. Num. Meth. Eng.* 2013, Vol. 93, No. 2, P. 160–182.

14. Rah K., Van Paepegem W., Habraken A. M., Degrieck J. A partial hybrid stress solid-shell element for the analysis of laminated composites. *Comp. Meth. Appl. Mech. Eng.* 2011, Vol. 200, No. 49–52, P. 3526–3539.

15. Kara N., Kumbasar N. Three-dimensional finite element for thick shells of general shape. *Int. J. for Physical and Engineering Sciences*. 2001, Vol. 52, P. 1–7.

16. Sze K. Y. Three-dimensional continuum finite element models for plate / shell analysis. *Prog. Struct. Eng. Mater.* 2002, Vol. 4, P. 400–407.

17. Caliri M. F., Ferreira A. J. M., Tita V. A review on plate and shell theories for laminated and sandwich structures highlighting the Finite Element Method. *Composite Structures.* 2016, Vol. 156, P. 63–77.

18. Matveev A. D., Grishanov A. N. [Multi-grid modeling of three-dimensional composite cylindric panels and shells]. *Materialy X mezhdunarodnoi konferentsii "Setochnye metody dlya kraevykh zadach I prilozheniya" – Materials of Xth International conference "Grid methods for boundary tasks and applications".* Kazan, 2014, P. 459–467 (In Russ.).

19. Matveev A. D., Grishanov A. N. [Two-grid modeling of cylindric shells and panels with variable thickness]. *Vestnik KrasGAU.* 2014, No. 4, P. 90–96 (In Russ.).

20. Matveev A. D., Grishanov A. N. [Multigrid curvilinear elements in three-dimensional analysis of cylindrical composite panels with cavities and holes]. *Uchenye zapiski Kazanskogo universiteta. 2014, Tom 156, Seriya: Fiziko-matematicheskie nauki.* 2014, Vol. 156, Book 4, P. 47–59 (In Russ.).

21. Kabanov V. V., Zheleznov L. P. [To the calculation of a cylindrical shell by the finite element method]. *Prikladnaya mekhanika*. 1985, Vol. 21, No. 9, P. 35–40 (In Russ.).

Библиографические ссылки

1. Зенкевич О. Метод конечных элементов в технике. М. : Мир, 1975. 544 с.

2. Норри Д., Де Фриз Ж. Введение в метод конечных элементов. М. : Мир, 1981. 304 с.

3. Голованов А. И., Тюленева О. И., Шигабутдинов А. Ф. Метод конечных элементов в статике и динамике тонкостенных конструкций. М. : Физматлит, 2006. 392 с.

4. Клочков Ю. В., Николаев А. П., Шубович А. А. Анализ напряженно-деформированного состояния оболочек вращения в геометрически нелинейной постановке при различных вариантах интерполяции перемещений. Волгоград : Волгоградский ГАУ, 2013. 152 с.

5. Киселев А. П. Расчет тонких оболочек на прочность в трехмерной постановке без упрощающих гипотез // Изв. вузов. Строительство. 2008. № 1. С. 18–23.

6. Киселев А. П., Гуреева Н. А., Киселева Р. З. Расчет многослойных оболочек вращения и пластин с использованием объемных конечных элементов // Изв. вузов. Строительство. 2010. № 1. С. 106–112.

7. Бате К., Вилсон Е. Численные методы анализа и метод конечных элементов. М. : Стройиздат, 1982. 448 с.

8. Болотин В. В., Новичков Ю. Н. Механика многослойных конструкций. М. : Машиностроение, 1980. 375 с.

9. Голушко С. К., Немировский Ю. В. Прямые и обратные задачи механики упругих композитных пластин и оболочек вращения. М. : Физматлит, 2008. 432 с.

10. Ahmed A., Kapuria S. A four-node facet shell element for laminated shells based on the third order zigzag theory // Composite Structures. 2016. Vol. 158. P. 112–127.

11. Carrera E., Pagani A. Valvano S. Shell elements with through-the-thickness variable kinematics for the analysis of laminated composite and sandwich structure // Composites. Part B: Engineering. 2017. Vol. 111. P. 294–314.

12. Yasin M. Y., Kapuria S. An efficient layerwise finite element for shallow composite and sandwich shells // Composite Structures. 2013. Vol. 98. P. 202–214.

13. Cinefra M., Carrera E. Shell finite elements with different through-the-thickness kinematics for the linear analysis of cylindrical multilayered structures // Int. J. Num. Meth. Eng. 2013. Vol. 93, No. 2. P. 160–182.

14. A partial hybrid stress solid-shell element for the analysis of laminated composites / K. Rah [et al.] // Comp. Meth. Appl. Mech. Eng. 2011. Vol. 200, No. 49–52. P. 3526–3539.

15. Kara N., Kumbasar N. Three-dimensional finite element for thick shells of general shape // Int. J. for Physical and Engineering Sciences. 2001. Vol. 52. P. 1–7.

16. Sze K. Y. Three-dimensional continuum finite element models for plate / shell analysis // Prog. Struct. Eng. Mater. 2002. Vol. 4. P. 400–407.

17. Caliri M. F., Ferreira A. J. M., Tita V. A review on plate and shell theories for laminated and sandwich structures highlighting the Finite Element Method // Composite Structures. 2016. Vol. 156. P. 63–77.

18. Матвеев А. Д., Гришанов А. Н. Многосеточное моделирование трехмерных композитных цилиндрических панелей и оболочек // Сеточные методы для краевых задач и приложения : материалы X Междунар. конф. Казань, 2014. С. 459–467.

19. Матвеев А. Д., Гришанов А. Н. Двухсеточное моделирование цилиндрических оболочек и панелей переменной толщины // Вестник КрасГАУ. 2014. № 4. С. 90–96.

20. Матвеев А. Д., Гришанов А. Н. Многосеточные криволинейные элементы в трехмерном анализе цилиндрических композитных панелей с полостями и отверстиями // Ученые записки Казанского ун-та. Сер. «Физ.-матем. науки». 2014. Т. 156, кн. 4. С. 47–59.

21. Кабанов В. В., Железнов Л. П. К расчету цилиндрической оболочки методом конечных элементов // Прикладная механика. 1985. Т. XXI, № 9. С. 35–40.